

Article

Detailed Assessment of the Effects of Meteorological Conditions on PM₁₀ Concentrations in the Northeastern Part of the Czech Republic

Vladimíra Volná^{1,2,*}  and Daniel Hladký¹

¹ Czech Hydrometeorological Institute, Na Šabatce 17, 143 06 Praha, Czech Republic; daniel.hladky@chmi.cz

² University of Ostrava, Faculty of Science, Department of Physical Geography and Geoecology, 30. dubna 22, 701 03 Ostrava, Czech Republic

* Correspondence: vladimira.volna@chmi.cz

Received: 6 April 2020; Accepted: 9 May 2020; Published: 12 May 2020



Abstract: This article assessed the links between PM₁₀ pollution and meteorological conditions over the Czech-Polish border area at the Třinec-Kosmos and Věřňovice sites often burdened with high air pollution covering the years 2016–2019. For this purpose, the results of the measurements of special systems (ceilometers) that monitor the atmospheric boundary layer were used in the analysis. Meteorological conditions, including the mixing layer height (MLH), undoubtedly influence the air pollution level. Combinations of meteorological conditions and their influence on PM₁₀ concentrations also vary, depending on the pollution sources of a certain area and the geographical conditions of the monitoring site. Generally, the worst dispersion conditions for the PM₁₀ air pollution level occur at low air temperatures, low wind speed, and low height of the mixing layer along with a wind direction from areas with a higher accumulation of pollution sources. The average PM₁₀ concentrations at temperatures below 1 °C reach the highest values on the occurrence of a mixing layer height of up to 400 m at both sites. The influence of a rising height of the mixing layer at temperatures below 1 °C on the average PM₁₀ concentrations at Třinec-Kosmos site is not as significant as in the case of Věřňovice, where a difference of several tens of $\mu\text{g}\cdot\text{m}^{-3}$ in the average PM₁₀ concentrations was observed between levels of up to 200 m and levels of 200–300 m. The average PM₁₀ hourly concentrations at Třinec-Kosmos were the highest at wind speeds of up to $0.5\text{ m}\cdot\text{s}^{-1}$, at MLH levels of up to almost 600 m; at Věřňovice, the influence of wind speeds of up to $2\text{ m}\cdot\text{s}^{-1}$ was detected. Despite the fact that the most frequent PM₁₀ contributions come to the Třinec-Kosmos site from the SE direction, the average maximum concentration contributions come from the W–N sectors at low wind speeds and MLHs of up to 400 m. In Věřňovice, regardless of the prevailing SW wind direction, sources in the NE–E sector from the site have a crucial influence on the air pollution level caused by PM₁₀.

Keywords: mixing layer height; ceilometer; suspended particulate matter; air pollution; Czech-Polish border

1. Introduction

PM₁₀ is a problematic pollutant with a wide spectrum of effects on human health, mostly on the respiratory and cardiovascular systems of the human body. The hazards of this pollutant lie not only in its quantity, thus in high measured concentrations, but also in the morphology of the particles and their qualitative composition. The suspended particulate matter is capable of creating bonds, which may, of course, result in transferring a range of other elements, e.g., heavy metals and polycyclic aromatic hydrocarbons, into the human body. The effects on the human body have clinically proven to be negative, especially in the form of carcinogenesis [1–5], for some of these transported substances.

As for the areas of concern, the areas in Europe most polluted by suspended particulate matter are the Po Valley in northern Italy, the countries of Eastern Europe, including the Balkan Peninsula, and part of Central Europe. The southern rim of the area (of Central Europe) occupies the northeastern part of the Czech Republic, and spreads northwards (in terms of area) to the larger territory of Poland [6,7]. This Czech-Polish region is part of the Upper Silesian Basin, which is a black coal basin of European significance. The first (primitive) black coal mining in the Upper Silesian Basin began as early as 1657 on Polish territory south of Katowice; real industrial mining development started in the Czech part of the basin no earlier than the second half of the 19th century [8]. The mining industry became the basis for the development of other industrial branches. In the entire region of the Upper Silesian Basin, there is an intricately interconnected system of industry, traffic infrastructure, and high density of population with individual solid fuel heating, which is historically related to black coal burning. All of the transborder region of the Silesian Voivodeship in Poland and the Moravian-Silesian Region in the Czech Republic rank among the most urbanized and industrialized regions in Europe [9,10]. All these anthropogenic activities negatively influence all the environmental components, and pronounced changes in these components have been recorded since the 1970s. From the point of view of air quality improvement, there were significant positive changes in the 1990s during the economic restructuring of both post-communist countries (Poland and the then-Czechoslovakia). Another major step forward was the accession of both countries to the European Union and the necessity of adapting their legislation to the EU requirements [11,12]. Owing to the mentioned measures, there has been a decrease in the pollution load of the Czech-Polish region; the problems, however, remain, and the exceedance of the pollution limits is still frequent [13,14]. This especially concerns the suspended particulate matter and benzo(a)pyren [15].

The particular air pollution level in the region of concern does not depend solely on the pollution source characteristics or the amount of discharged pollutants, but also on the physical geography and meteorological conditions of the area in question. It is the meteorological conditions themselves that determine the intensity and manner of the dispersion of contaminants [16]. The wind direction and speed and the vertical atmospheric stability, contingent on the air temperature, are considered the most important and decisive meteorological dispersion conditions. The wind characteristics influence the transport of pollutants in the horizontal direction, the atmospheric stability and the air temperature influence the dispersion of pollutants in the vertical direction. In the most stable situations, the air temperature rises with the height and the conditions for the vertical mixing are the worst. Conversely, at unstable stratification, the temperature drops more quickly than it would under regular conditions in the atmosphere, and the conditions for pollutant dispersion are favorable [17–19].

It is possible to express the dispersion conditions numerically using the ventilation index, which is defined as a product of the mixing layer height and the average wind speed in the mixing layer [20]. A situation with unfavorable dispersion conditions does not always have to mean the occurrence of high contaminant concentrations. It is important to bear in mind the situation duration, the original pollution level, the source distribution, and the emissions into the layer under inversion. It is, however, possible to state that a significant exceedance of the allowed pollution limits occurs mostly in mildly unfavorable and unfavorable dispersion conditions, or due to the concurrence of other meteorological factors. In order to calculate the ventilation index, the ALADIN (Aire Limitée, Adaptation Dynamique, Development International) numerical forecast model is used in the Czech Republic; this model is meant mostly for short-term forecast composition [21]. It is also possible to find out the information about the atmospheric boundary layer and the mixing layer height by means of direct monitoring. Measurements using radiosondes, high masts, and special devices, such as SODARs (Sonic Detection and Ranging), LIDARs (Light Detection and Ranging), and wind profilers, are used. In the presented analysis, mixing layer height measurement results obtained by means of ceilometers were used. The higher the mixing layer height, the more intensive the mixing of air, and thus, the better the conditions are for contaminant dispersion [22,23].

Awareness of the links between PM_{10} concentrations and meteorological variables and their mutual combination is an important premise for assessment of the pollution situation and a possible pollutant concentration trend forecast [24–28]. The detection of these dependences is especially important for the assessment of complex situations with the occurrence of smog situations [29,30]. Apart from those pollutant concentrations exceeding the limit value, knowledge of the development of the meteorological situation, weather forecasts, and thus the possibilities for overall improvement or deterioration of the situation due to better or worse air pollutant dispersion, are important aspects for the announcement of smog situations. Improving the knowledge of correlations between the mostly high suspended particulate matter concentrations and the meteorological conditions may be a significant aspect for defining the measures preventing health hazards in the assessed densely populated region [31].

With this article, the authors reassume a similar topic of PM_{10} concentration dependences on the mixing layer height in the area of interest [32]. In the mentioned analysis, the measurement results were assessed at the Věřňovice, Třinec-Kosmos, and Mošnov/Studénka sites for the cold parts of the years 2016/2017 and 2017/2018. The differences in the established facts were caused mostly by a different site location (orography) and by the structure of the sources that influence the pollution. Pollutants other than PM_{10} and other meteorological variables were not included in the assessment.

The anticipated findings of this analysis shall be an understanding of the combinations of the meteorological conditions, the mixing layer height, and the connection to PM_{10} concentrations. The highest PM_{10} concentrations are generally reached at a low mixing layer height, low wind speed or calm air, and at a low air temperature. These assumptions correspond to previous results concerning the dependence of pollutant concentration on the mixing layer height in Europe [33–37]. Furthermore, the mixing layer height and its influence on the pollutant concentrations in the air have been written about in articles in Asia, e.g., in India [38] and China [39], which, as far as the comparability of pollution-meteorology correlations is concerned, is hardly transferrable, given these significantly different areas. The reasons are the different climatological conditions between the Czech-Polish border area and Asia, specifically the meteorological and geographical conditions of the selected locations, the air pollution intensity, and the different position and types of air pollution sources with respect to the monitored ambient air quality stations. The wind direction and speed, as well as the mixing layer height, also make it possible, at least in part, to reveal the main air pollution sources in the monitored border locations. With regard to a different area relief in which the monitored locations are situated, it has been assumed that the PM_{10} concentration dependences on meteorological variables are bound to differ up to a certain point.

2. Experiments

For the assessment, sites of the Czech Hydrometeorological Institute [40] have been chosen—Třinec-Kosmos [41] and Věřňovice [42], located in the northeastern part of the Moravian-Silesian Region of the Czech Republic (Figure 1). The monitored sites are about 34 km apart in a straight line. Both sites belong to the National Air Quality Monitoring Network of the Czech Republic [43]. At the Třinec-Kosmos and Věřňovice sites, PM_{10} concentrations are measured by means of a radiometric method based on the absorption of beta radiation in a sample collected on filter material by means of an Automatic suspended particulate monitor MP101M [44]. The wind direction and speed are measured at a standard height of 10 m by means of a WindSonic machine, based on ultrasound technology. The air temperature is scanned at a height of 2 m above the ground, by means of a Cormet company machine. At both sites, special ceilometer devices are placed that are traditionally used to measure the height of the cloud base and the cloud amount in individual layers, the vertical visibility, and the aerosol concentration in the ground atmospheric layer. These ceilometers contain a presentation module that enables the measurement and display of the structure of the atmospheric boundary layer based on an algorithm that determines the thickness of the mixing layer depending on the aerosol concentration in the atmosphere. In both cases, these are Vaisala CL31 Ceilometers [45].

It is necessary to point out that measurement by means of ceilometers is limited by height. Although the upper measurement limit reaches the height of a few kilometers, it is impossible to regard the Earth's surface level as the bottom limit. In the vicinity of the Earth's surface, the measurement is limited by higher noise that can reach up to a height of 50 m [46].

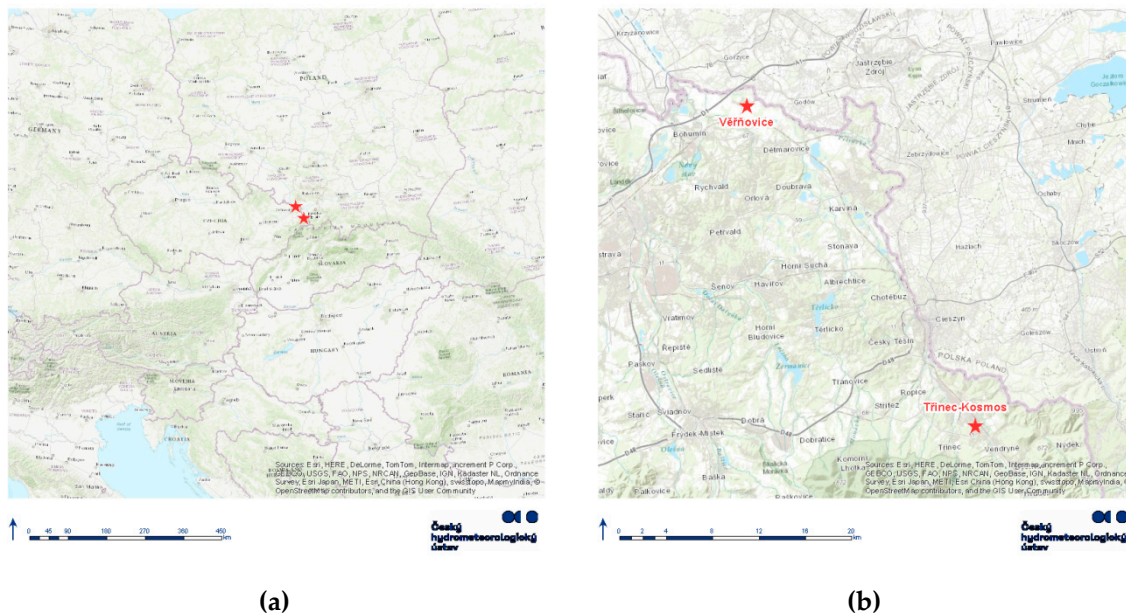


Figure 1. The assessed site location: (a) The location within Central Europe; (b) The location within the Czech-Polish border region.

For the purposes of the analysis, the average hourly values of the mixing layer height were used, calculated from the data measured at 16-second intervals from the ceilometers at the Třinec-Kosmos and Věřňovice sites. The output hourly values of PM_{10} , temperature, wind speed, and direction were also used in the analysis. Due to large diurnal mixing layer height (MLH) variation, the analysis also included the daily averages of the parameters. Correlation coefficients in the analysis are calculated from the hourly and daily data in relation to the MLH, which was divided into 20 intervals and, subsequently, from their arithmetic means and medians. In the case of daily MLH averages, intervals from a height of 150 m are available. The assessed period is from 2016 to 2019. The data utilization rate used for the monitored period was high. In the case of hourly data on PM_{10} and meteorological variables (air temperature, wind direction, and speed) the average at both sites is 98%; it is 87% from the ceilometers' data for the mixing layer height. In order to assess higher PM_{10} concentrations and exceedance numbers, a limit value of $50 \mu\text{g}\cdot\text{m}^{-3}$ was purposefully chosen, which corresponds to the value of the daily pollution limit for PM_{10} [13]. The term “cold period of the year” is used for the months of January through March and October through December; the term “warm period of the year” is used for the months of April through September.

In the analysis, concentration roses were also used for illustrative purposes, which show average PM_{10} concentrations for the given wind direction and speed, as well as weighted concentration roses [47]. The difference between a concentration rose and a weighted concentration rose is that the latter provides information about how often a given wind direction and speed combination occurs and states to what extent the concentrations detected for a given wind speed and direction affect the overall average concentration for a given period. The comparison of the two roses may show a significant pollution source located, however, in a sector from which the wind only rarely blows and thus does not contribute significantly to the overall average concentration. The concentration rose reveals what the pollution situation was at maximum concentrations of a given contaminant at a particular site; the weighted concentration rose shows from what wind direction and at what speed the pollution came to the largest extent for the whole period. For the above-described reasons, both rose types for

the same site and period may vary significantly [48]. In the presented roses, there is information about calm air, which is a situation with a wind speed of $0\text{--}0.2\text{ m}\cdot\text{s}^{-1}$.

The Třinec-Kosmos site is situated in the center of the city of Třinec, in a typical residential development. In the immediate vicinity of the site there are a parking lot as well as a residential development type of road. In the northeastern (NE) direction from the site, the closest pollution line source is a frequented road with an average number of vehicles of more than 9000 every 24 h [49]. The Třinecké železářny a.s. industrial plant premises are situated in the northwestern (NW) sector about 1.5 km from the site. The closest housing development with individual heating is situated in the N–NE direction about 500 m from the site, another is in the S–SW direction about 1 km from the site. The shortest route towards the Polish border is in the NE direction about 3 km from the site. The Třinec-Kosmos site is situated at the end of the Jablunkov Furrow, which starts at Jablunkov Pass and separates the Moravian-Silesian and the Silesian Beskydy mountain ranges. The shortest distance to the foothills of the Beskydy mountains is just 4.5 km southwest of the station. In the furrow is the Olše River basin that drains off the surrounding undulating relief [50,51]. The direction of the furrow also determines the prevailing wind direction along the southeast/northwest axis (Figure 2a) [52]. In the vicinity of the site, at a distance of 40 m in the NE direction, there is a high-rise, a roughly 50-meter-high building that may, with regard to the prevailing wind direction, slightly muffle the wind influence from the northeast.

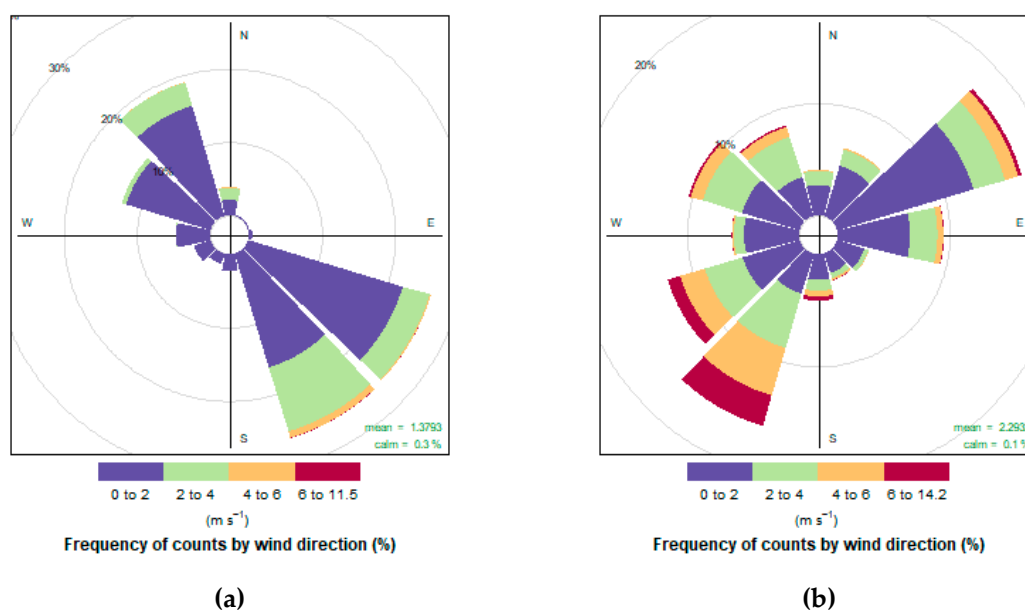


Figure 2. Average frequency of counts by wind speed and wind direction, 2016–2019: (a) Třinec-Kosmos; (b) Věřňovice.

According to the existing pollution assessment analyses of the Třinec-Kosmos site, apart from the significant contribution of secondary particles, a combination of sources from abroad and local heating and industry, as well as road traffic, contribute significantly to the PM_{10} concentrations [52]. At lower wind speeds of up to $2\text{ m}\cdot\text{s}^{-1}$, with a prevailing southeastern (SE) wind direction, a significant influence of dense housing development with individual heating is very likely to be seen at the site. Conversely, in situations with a NW wind direction, a significant influence of the industrial sources of Třinecké železářny is assumed, which includes both high- as well as low-emitting sources. At higher wind speeds, the influence of sources situated north of the site at a greater distance is also apparent here in the cold period of the year, which points at foreign sources from Poland.

The Věřňovice site is situated in the cadastral area of the Dolní Lutyně municipality, about 300 m east of the Věřňovice village and about 1 km south of the Czech-Polish border. In the immediate vicinity of the site, there is an infrequently used and partly paved road flanked by deciduous trees and

fields. Roughly 1.5 km in the NW direction, there is a highway with roughly 11,000 vehicles a day [49]. The closest significant industrial source, Elektrárna Dětmárovice a.s., is situated about 3 km southeast of the site. The Věřňovice site is situated in open terrain in the vicinity of the River Olše. At the site, the prevailing wind direction is along the southwest/northeast axis where the more frequent flow is southwest (Figure 2b). Věřňovice is situated in the area of the Ostrava Basin where the “Moravian Gate” ends; this divides the Podbeskydská hilly area and Nízký Jeseník [50,51]. The shape of the gate along the southwest/northeast axis significantly determines the prevailing wind direction of the region where Věřňovice is situated. It is apparent from the existing analyses that local fireplaces have the greatest contribution to the exceedance of PM₁₀ pollution limits here among the primary sources, mostly those used on the territory of Poland [52].

3. Results

The suspended particulate matter concentrations at both sites are assessed depending on the mixing layer height and other meteorological variables—air temperature, wind speed, and direction.

3.1. Dependence of Suspended Particulate Matter Concentrations on the Mixing Layer Height

Based on the average daily courses of hourly concentrations of PM₁₀ and MLH in the period between 2016 and 2019 for both stations, it is obvious that the lowest MLH is measured in the evening and night hours and the early morning hours (Figure 3). During this period, the highest PM₁₀ concentrations were observed at the Věřňovice station. In both cases, higher PM₁₀ concentrations were observed in the cold part of the year, when the daily variability was also greater than in the warm part of the year.

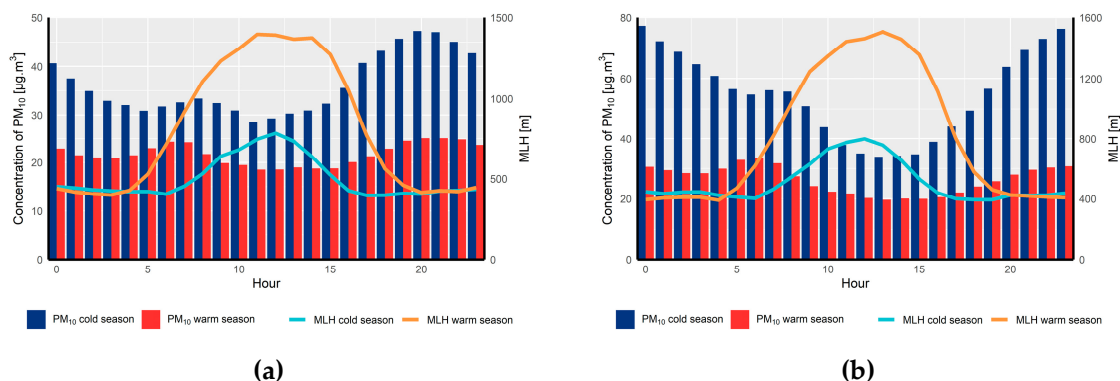


Figure 3. Daily course of hourly PM₁₀ concentrations and mixing layer height (MLH), 2016–2019: (a) Třinec-Kosmos; (b) Věřňovice.

The distribution of the PM₁₀ and MLH hourly values is depicted in Figure 4.

In order to work out the dependence of PM₁₀ concentrations on the mixing layer height over the period from 2016 to 2019, correlation coefficients have been calculated for the values of their averages and medians. The median calculations have been added for the purposes of comparison without the influence of extreme values. The highest mean and median hourly PM₁₀ concentrations at the Třinec-Kosmos station for the entire period between 2016–2019 were observed at MLHs of 150 to 300 m. At the Věřňovice station, the highest hourly concentrations were observed at the lowest MLH, below 200 m. Domestic heating, a low (in terms of height) source of air pollution with the typical chimney height below 15 m, has a significant effect at both locations. The Třinec-Kosmos station is also significantly affected by the large industrial site of Třinecké železářny (Třinec Ironworks), with a chimney height of 100 m or more. At MLHs below 300 m, there is an increase in PM₁₀ concentrations, due to emissions from both domestic heating and industrial sources. At lower MLHs, the emissions from higher chimneys spread above this height. At higher MLHs (below 300 m), both domestic heating emissions and nearby industrial sources are very significant. After comparing all the levels of MLH,

higher PM₁₀ concentration values occurred at Věřňovice than in Třinec-Kosmos. On the occurrence of higher levels of the mixing layer, lower PM₁₀ concentrations were reached at both sites (Figure 5). For the Třinec-Kosmos station, the correlation coefficient for the 2016–2019 period calculated from the mean hourly values of concentrations at increasing MLHs is -0.83 ; from the median values, it is -0.84 . The correlation coefficient from the mean daily values is -0.79 ; from the median values, it is -0.77 . At the Věřňovice station, the correlation coefficient from the mean hourly values for PM₁₀ in relation to the increasing MLH is -0.76 , and from the median values, it is -0.85 . The correlation coefficient at the Věřňovice station for the entire period from 2016 to 2019 from the mean daily values is -0.74 ; for the median values, it is -0.75 .

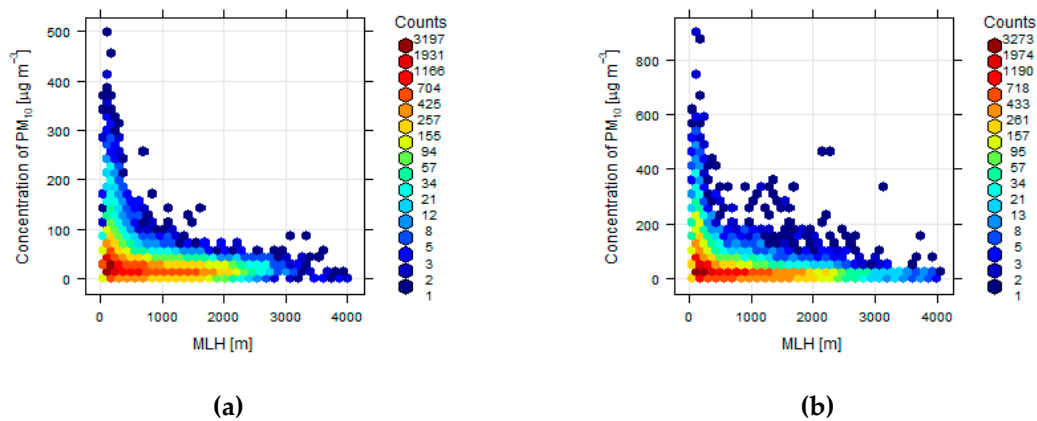


Figure 4. Hourly PM₁₀ concentration variability in relation to MLH, 2016–2019: (a) Třinec-Kosmos; (b) Věřňovice.

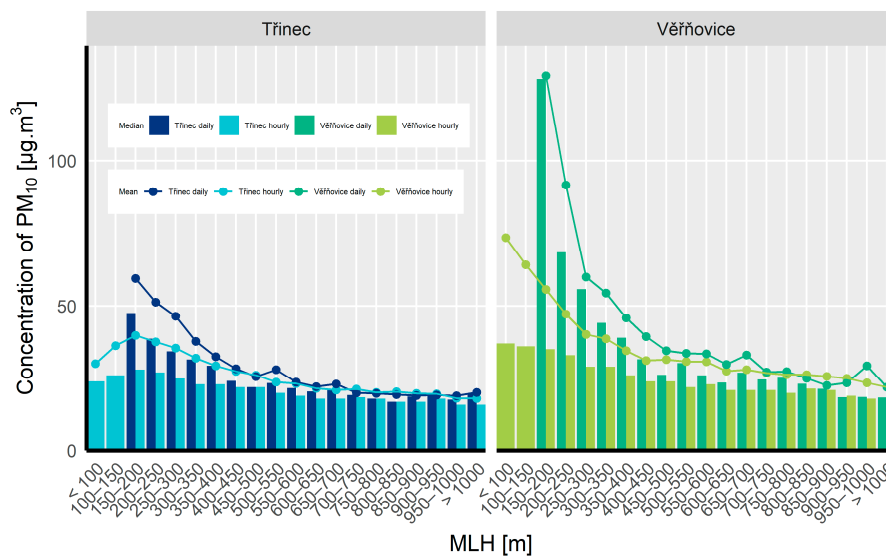


Figure 5. Mean and median PM₁₀ concentration values at mean and median MLH values, Třinec-Kosmos, Věřňovice, 2016–2019.

The correlation coefficients (hourly and daily values) of PM₁₀ dependences on MLH differ over the period from 2016 to 2019 at both sites; it is, however, possible to state that they are statistically significant dependences in all the cases (Table 1). When comparing the MLH arithmetic and median averages in the individual years, the highest values were reached in 2019 at both sites; they were higher at Věřňovice than at Třinec-Kosmos (Table 2).

Table 1. Correlation coefficients of PM₁₀ concentration dependences on MLH and the mixing layer height values at the Třinec-Kosmos and Věřňovice sites, 2016–2019.

Year	Třinec-Kosmos				Věřňovice			
	Hour		Day		Hour		Day	
	Arithmetic Mean	Median						
2016	−0.85	−0.83	−0.81	−0.78	−0.76	−0.84	−0.70	−0.66
2017	−0.81	−0.83	−0.84	−0.81	−0.80	−0.90	−0.72	−0.69
2018	−0.81	−0.85	−0.79	−0.81	−0.82	−0.87	−0.81	−0.79
2019	−0.84	−0.84	−0.72	−0.69	−0.64	−0.78	−0.73	−0.85

Table 2. The mixing layer height values at the Třinec-Kosmos and Věřňovice sites, 2016–2019.

Year	Třinec-Kosmos		Věřňovice	
	Arithmetic Mean (m)	Median (m)	Arithmetic Mean (m)	Median (m)
2016	604	369	555	327
2017	659	425	628	372
2018	675	450	670	408
2019	705	501	821	553

3.2. Dependence of the Suspended Particulate Matter Concentrations on the Mixing Layer Height and the Air Temperature

The distribution of temperature and MLH hourly values are depicted in Figure 6.

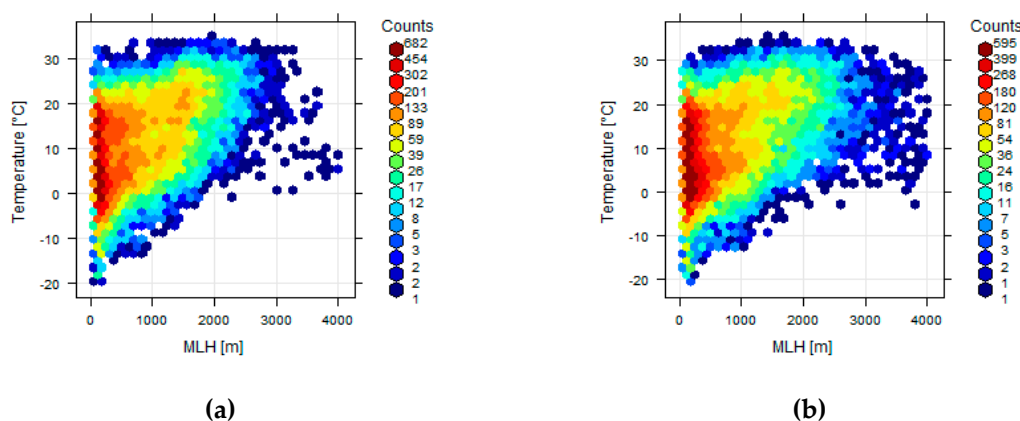


Figure 6. Variation of hourly temperature values in relation to MLH, 2016–2019: (a) Třinec-Kosmos; (b) Věřňovice.

The lowest average and median temperature values (hourly and daily values) were reached at both sites over the whole period from 2016 to 2019 on the occurrence of MLHs of 150 up to 300 m. From an MLH of 300 m the mean temperature values rise with increasing MLHs (or range around similar values) and the highest values are observed at an MLH above 800 m (Figure 7). On average, the statistical dependency expressed by a correlation coefficient between the temperature and MLH is significant over the whole period from 2016 to 2019 at both sites. The correlation coefficients calculated from the mean and median values (from the hourly and daily data) range between 0.85 and 0.94 on average for the entire period of analysis for both stations.

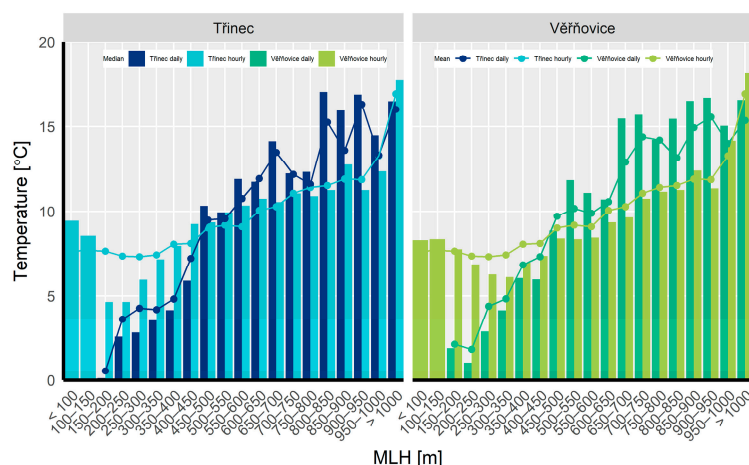


Figure 7. Mean and median temperature values at mean and median MLH values, Třinec-Kosmos, Věřňovice, 2016–2019.

The correlation dependences between the temperature and the mixing layer height changed over the years of 2016 to 2019 at both sites. The correlation dependence is significant every year of the monitored period (Table 3).

Table 3. Correlation coefficients of dependences of the temperature on the MLH at the Třinec-Kosmos and Věřňovice sites, 2016–2019.

Year	Třinec-Kosmos				Věřňovice			
	Hour		Day		Hour		Day	
	Arithmetic Mean	Median						
2016	0.95	0.88	0.89	0.81	0.94	0.87	0.89	0.90
2017	0.92	0.84	0.92	0.94	0.96	0.91	0.88	0.89
2018	0.90	0.82	0.88	0.90	0.93	0.84	0.93	0.89
2019	0.96	0.92	0.85	0.82	0.91	0.79	0.86	0.75

The PM₁₀ concentrations are significantly dependent on the mixing layer height and temperature in the case of both sites over the entire monitored period from 2016 to 2019. The average PM₁₀ concentrations reach their highest values at temperatures below 1 °C. At the Třinec-Kosmos location, the highest average daily and hourly PM₁₀ concentrations were observed at temperatures below 1 °C and a mixing layer height lower than 200 to 300 m. At temperatures above 5 °C, the average daily PM₁₀ concentrations were highest at an MLH between 200 and 300 m. At a higher MLH the PM₁₀ concentration values were almost identical. The average daily and hourly PM₁₀ concentrations at the Věřňovice station reached the highest values during the entire period of analysis in combination with the relationship between the temperature and height of the mixing layer, at temperatures below 1 °C and a mixing layer height below 200 m. At the same temperature, but at an MLH of 200–300 m, the average daily concentrations were lower, but still double the limit value of 50 µg·m⁻³. A more significant PM₁₀ concentration dependence on temperature as well as MLH was observed at Věřňovice. At Třinec, a lower temperature had a substantial influence on PM₁₀ concentrations; the mixing layer height influence was shown mostly up to an MLH of 400 m. The combination of a low temperature and low MLH level corresponds to the general assumption about the occurrence of poorer dispersion conditions in the cold period of the year as opposed to the assumed occurrence of better dispersion conditions in the warm period of the year (Figures 8a and 9a). When observing the correlations among the numbers of exceedances of PM₁₀ daily concentration values of 50 µg·m⁻³ and the MLH and temperature (Figures 8b and 9b), a decreasing count of exceedances of this value is apparent with

a rising temperature and increasing MLH. The highest number of $50 \mu\text{g}\cdot\text{m}^{-3}$ value exceedances for PM_{10} daily concentrations is observed at temperatures below 1°C and MLHs below 300 m. For both sites, a slight increase in the number of 1-hour PM_{10} concentrations above $50 \mu\text{g}\cdot\text{m}^{-3}$ is apparent at an MLH level above 1000 m as opposed to 800 to 1000 m.

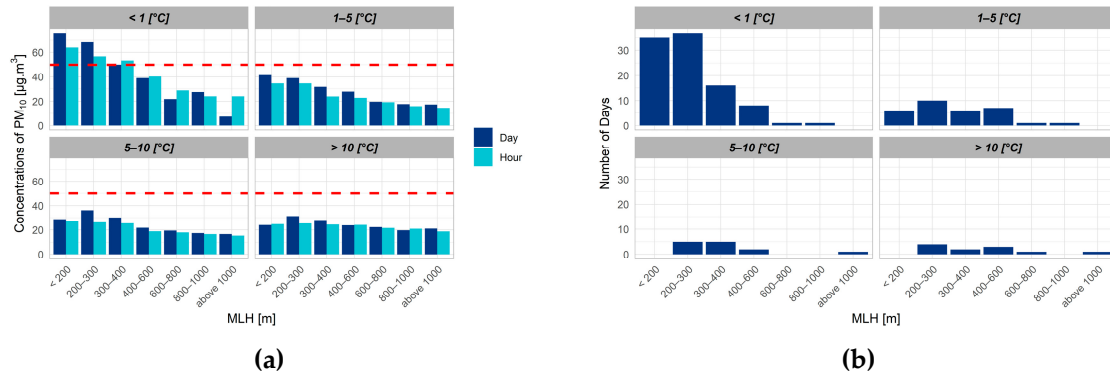


Figure 8. The Třinec-Kosmos site, 2016–2019: (a) Average PM_{10} concentrations depending on the mixing layer height and temperature; (b) Exceedance count of daily concentrations of $50 \mu\text{g}\cdot\text{m}^{-3}$ depending on the mixing layer height and temperature.

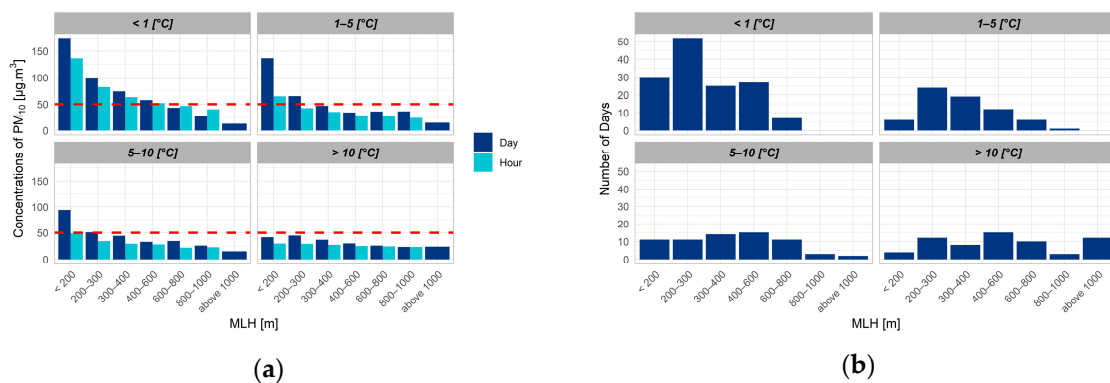


Figure 9. The Věřňovice site, 2016–2019: (a) Average PM_{10} concentrations depending on the mixing layer height and temperature; (b) Exceedance count of daily concentrations of $50 \mu\text{g}\cdot\text{m}^{-3}$ depending on the mixing layer height and temperature.

3.3. Dependence of Suspended Particulate Matter Concentrations on the Mixing Layer Height, Wind Speed, and Direction

The distribution of wind speed and MLH hourly values are depicted in Figure 10.

At the Třinec-Kosmos site, a wind speed measured at 10 m does not significantly change with a rising MLH. At the Věřňovice site, the wind speed change is more apparent with a rising MLH. Here, the difference of the average values of the wind speed on the occurrence of MLH levels of up to 200 m and above 400 m makes up 1 and more $\text{m}\cdot\text{s}^{-1}$ (Figure 11). The correlation dependences of the wind speed on MLH are low at the Třinec-Kosmos site; the Věřňovice site shows a statistically more significant dependence than the Třinec-Kosmos site. Higher wind speeds are observed at the Věřňovice station, compared to the Třinec-Kosmos station. The differences are due to the more complex orography of the Třinec region compared to the relatively flat and open region surrounding Věřňovice. The station in Třinec is located in a housing development, at the foothills of the Beskydy Mountains (Chapter 2). This means that the correlation between MLH and wind speed at the Třinec-Kosmos station is much less significant or even insignificant, compared to the station in Věřňovice.

The correlation dependences of the wind speed and MHL also differ from site to site throughout the years of the assessed period. A statistically more significant dependence of the wind speed on the MLH is apparent at the Věřňovice site (Table 4).

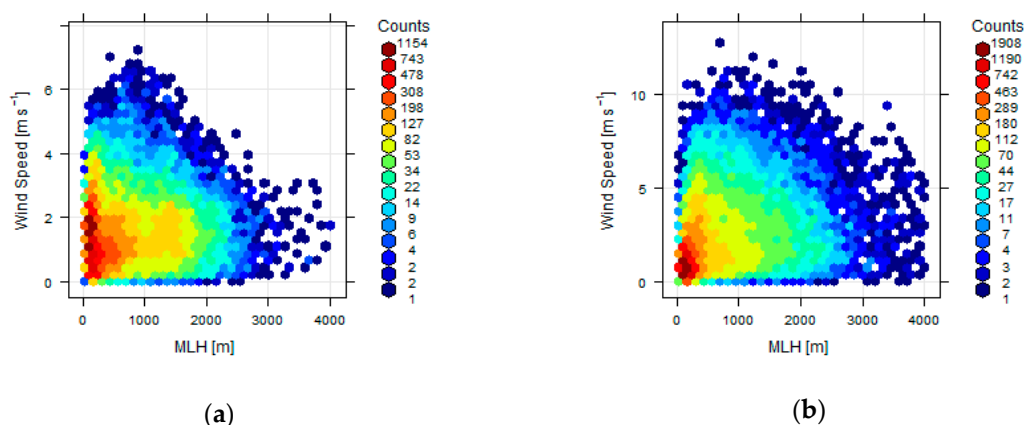


Figure 10. Variation of hourly wind speed values in relation to MLH, 2016–2019: (a) Třinec-Kosmos; (b) Věřňovice.

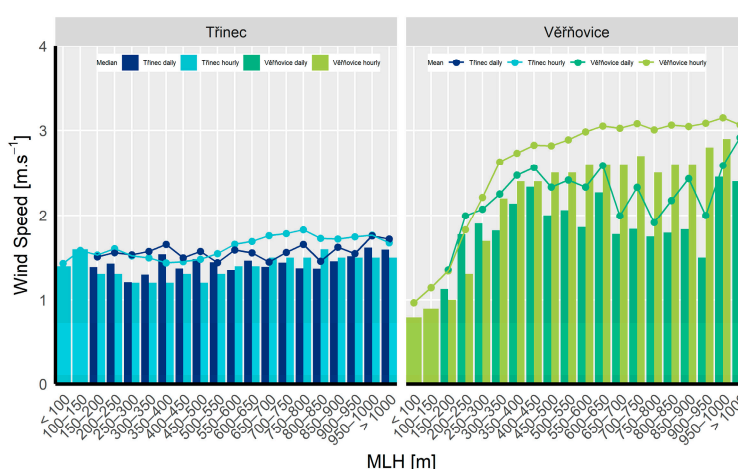


Figure 11. Average and median values of the wind speed at average and median MLH values, Třinec-Kosmos, Věřňovice, 2016–2019.

Table 4. Correlation coefficients of dependences of the wind speed on the MLH, Třinec-Kosmos and Věřňovice, 2016–2019.

Year	Třinec-Kosmos				Věřňovice			
	Hour		Day		Hour		Day	
	Arithmetic Mean	Median						
2016	0.53	0.45	0.28	0.32	0.69	0.69	0.07	0.32
2017	0.56	0.41	0.46	0.55	0.79	0.79	0.53	0.49
2018	0.60	0.53	0.1	0.27	0.75	0.76	0.52	0.35
2019	0.51	0.34	0.01	0.2	0.63	0.71	0.43	0.37

PM₁₀ concentrations are significantly dependent on the MLH and wind speed. At the Třinec-Kosmos site, situations with calm air and wind speeds of up to 0.5 m·s⁻¹ had an apparent influence on higher hourly PM₁₀ concentrations. At wind speeds between 0.5–2 m·s⁻¹, the highest average hourly concentrations were observed at MLHs of 200–300 m. The average daily PM₁₀ concentrations were always the highest at MLHs below 200 m. Average daily wind speeds below 0.5 m·s⁻¹ were not available for the two stations of interest (Třinec-Kosmos and Věřňovice). The daily average wind speed values were 0.5 m·s⁻¹ or more. The influence of the wind speed on PM₁₀ concentrations decreased with the mixing layer height at the Třinec-Kosmos site. At wind speeds above 2 m·s⁻¹, the PM₁₀ concentrations were lowest at the site. During the observation of the occurrence

of the hourly PM_{10} concentrations above $50 \mu\text{g}\cdot\text{m}^{-3}$, the highest count of these higher values was undoubtedly at wind speeds of $1\text{--}2 \text{ m}\cdot\text{s}^{-1}$ and $0.5\text{--}1 \text{ m}\cdot\text{s}^{-1}$ and MLHs of up to 300 m. The lowest number of daily PM_{10} concentrations above $50 \mu\text{g}\cdot\text{m}^{-3}$ was observed at wind speeds above $2 \text{ m}\cdot\text{s}^{-1}$ and MLHs above 400 m (Figure 12).

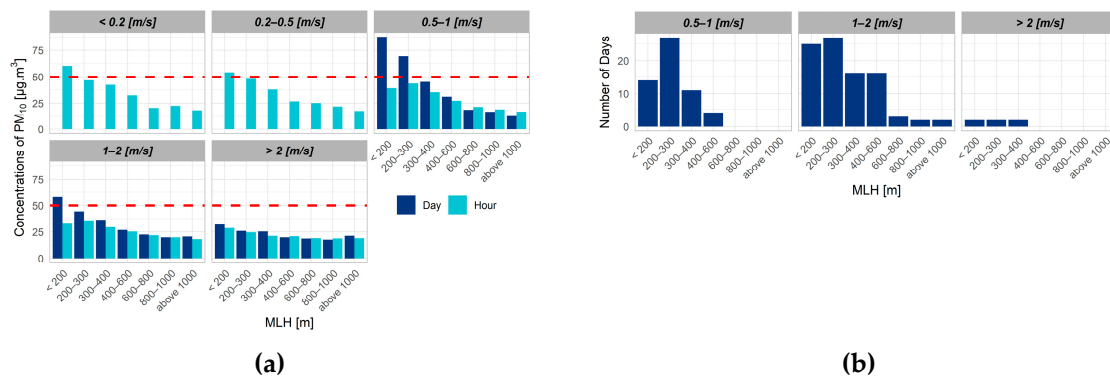


Figure 12. The Trinec-Kosmos site, 2016–2019: (a) Average PM_{10} concentrations depending on the mixing layer height and wind speed; (b) The count of exceedances of daily concentrations of $50 \mu\text{g}\cdot\text{m}^{-3}$ depending on the mixing layer height and wind speed.

The situation at the Věřňovice site was slightly different. The highest average hourly PM_{10} concentrations were observed at MLHs below 200 m and wind speeds between $0.5\text{--}2 \text{ m}\cdot\text{s}^{-1}$, or under calm conditions and wind speeds below $0.5 \text{ m}\cdot\text{s}^{-1}$. The highest average daily PM_{10} concentrations were observed at MLHs below 200 m and wind speeds below $2 \text{ m}\cdot\text{s}^{-1}$. The lowest average PM_{10} concentrations were reached at all levels with the highest wind speeds above $2 \text{ m}\cdot\text{s}^{-1}$. The highest number of $50 \mu\text{g}\cdot\text{m}^{-3}$ value exceedances for PM_{10} daily concentrations was observed at wind speeds between 1 and $2 \text{ m}\cdot\text{s}^{-1}$ and MLHs of 200 to 300 m, at lower wind speeds below $1 \text{ m}\cdot\text{s}^{-1}$, and MLHs below 200 m (Figure 13).

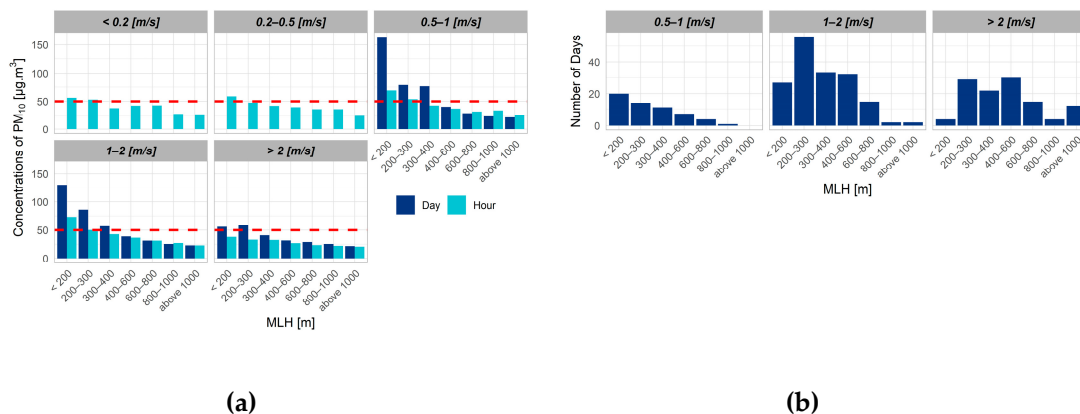


Figure 13. The Věřňovice site, 2016–2019: (a) Average PM_{10} concentration depending on the mixing layer height and wind speed; (b) The count of exceedances of daily concentrations of $50 \mu\text{g}\cdot\text{m}^{-3}$ depending on the mixing layer height and wind speed.

The prevailing wind directions vary noticeably over the whole period from 2016 to 2019 at both sites (Figure 14). At the Trinec-Kosmos site, the prevailing wind direction is along the southeast/northwest axis, where the SE wind direction prevails. The average relative frequencies of counts of wind directions changed in the individual months throughout the whole period; the prevailing SE wind direction, however, remained. The least frequent wind direction was NE. At the Věřňovice site, the highest frequency of counts of the wind direction is along the southwest/northeast axis; the frequencies of counts of the prevailing wind direction, however, differed throughout the year. On average, the southwestern

(SW) wind direction prevailed in the cold months (October to March). In the warm part of the year, the NE and NW wind directions prevailed. The SE wind direction at the Věřňovice site was the least frequent throughout the whole monitored period.

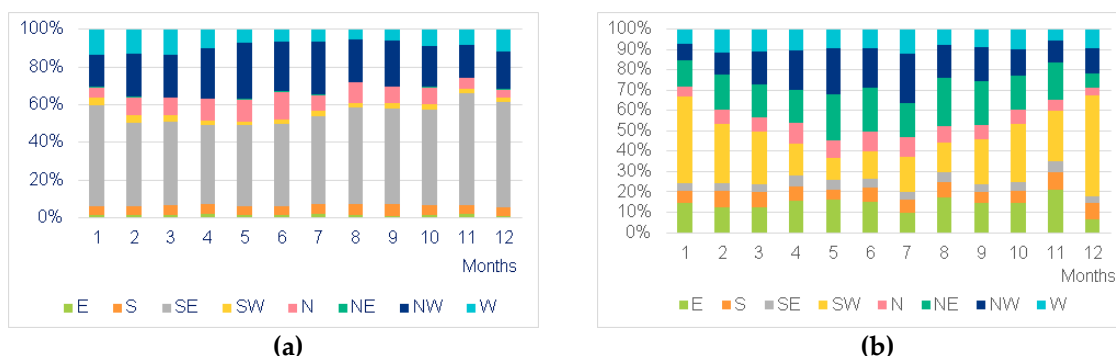


Figure 14. Relative frequency of counts of wind direction representation, 2016–2019: (a) the Trinec-Kosmos site; (b) the Věřňovice site.

The average monthly PM₁₀ concentrations reached the highest values at the lowest average MLH in the cold months of the year at all wind directions at Trinec-Kosmos. The lowest average monthly PM₁₀ concentrations were reached during the SE wind direction. During the SE and E wind directions, the MLHs also reached the lowest values of the average monthly heights of the mixing layer. In comparing the years from 2016 to 2019, it is apparent that on average, 2019 showed higher values of the mixing layer height than the preceding years, which is also reflected in the lower average PM₁₀ concentrations (Figure 15).

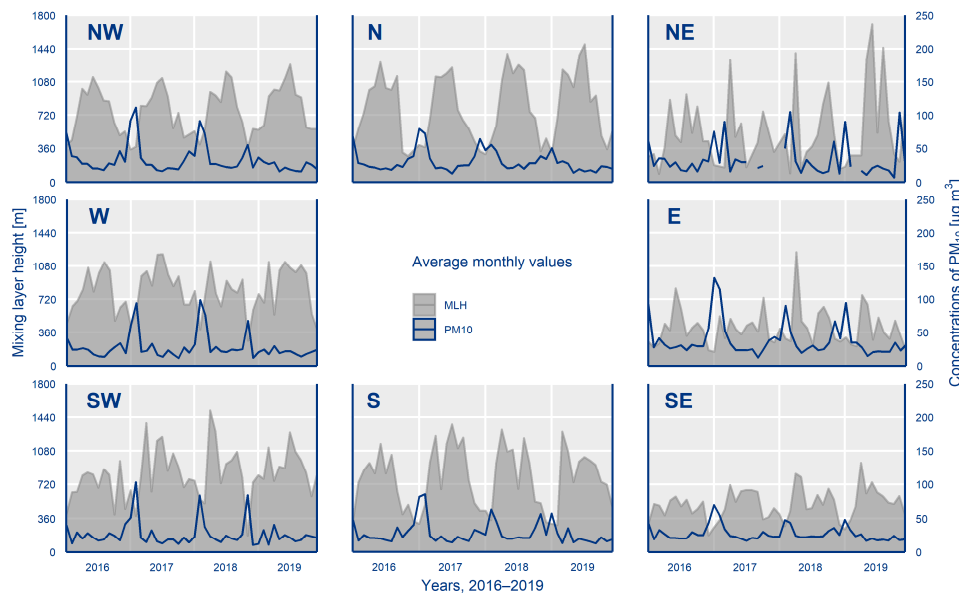


Figure 15. Average PM₁₀ concentrations depending on the mixing layer height and wind direction, the Trinec-Kosmos site, 2016–2019.

The weighted concentration roses for PM₁₀ divided according to the mixing layer height (Figure 16) show that the most frequent contribution to the average PM₁₀ concentrations for the period from 2016 to 2019 comes to the Trinec-Kosmos site from a southeasterly direction, which basically corresponds to the described prevailing wind directions at this location. This information, however, does not necessarily mean that the maximum PM₁₀ concentration contributions also come from the same direction; winds from other directions can carry higher concentrations of PM₁₀, which may lead to the exceedance of the

daily limit of the pollution value for PM₁₀ of 50 µg·m⁻³. The division of the weighted concentration roses according to the mixing layer height describes the PM₁₀ concentration at the height of the ground measurement at the site when the mixing layer height reached various levels.

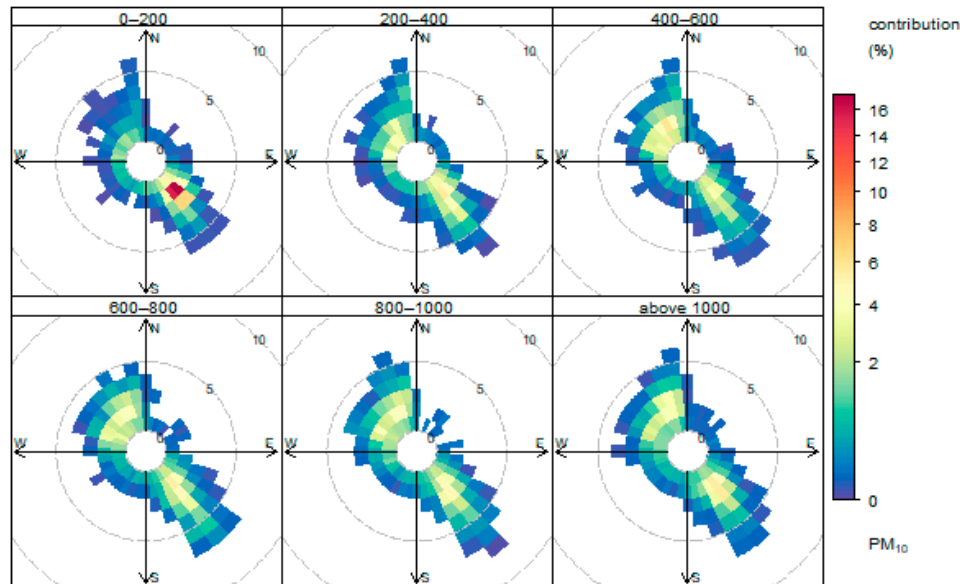


Figure 16. PM₁₀ weighted concentration rose divided according to the mixing layer height (in m), the Třinec-Kosmos site, 2016–2019.

The lowest MLHs at the Věřňovice site are registered for the NE and E wind directions, when the highest average PM₁₀ concentrations were reached over the entire period from 2016 to 2019. Conversely, the highest MLHs are reached during wind directions from the S to W sectors, when the lowest average monthly PM₁₀ concentrations occur during the SE and SW wind directions. Having compared the individual years, it becomes apparent that as well as at Třinec-Kosmos, the average MLH in 2019 was, on the whole, the highest, and the average PM₁₀ concentrations reached the lowest values of the entire monitoring period (Figure 17).

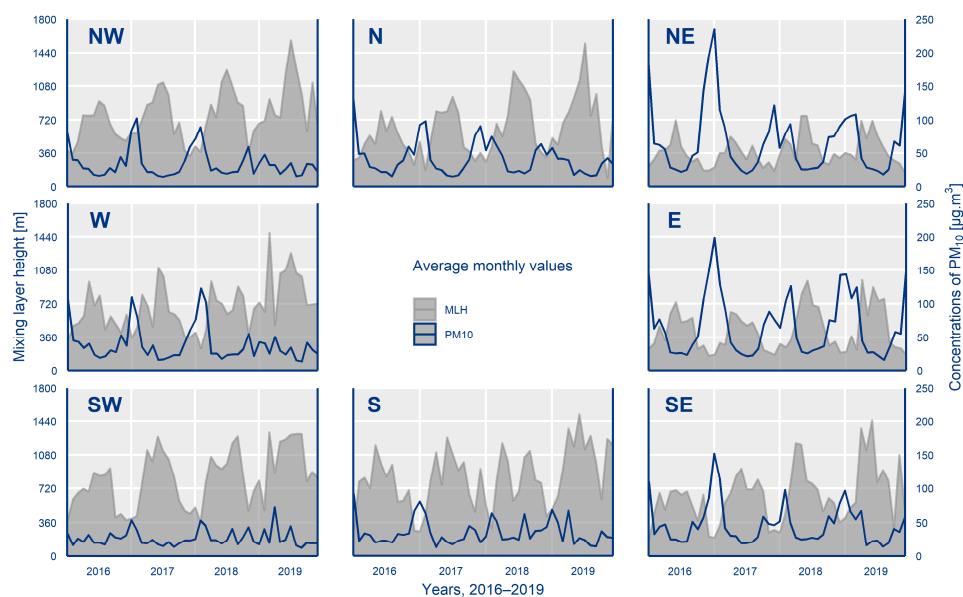


Figure 17. Average PM₁₀ concentrations depending on the mixing layer height and wind direction, the Věřňovice site, 2016–2019.

The weighted concentration roses for PM₁₀, divided according to the mixing layer height (Figure 18), show that the most frequent contribution to the average PM₁₀ concentrations for the period from 2016 to 2019 come to the Věřňovice site from the NE sector at wind speeds of up to 2 m·s⁻¹, despite the fact that, on the whole, the SW wind direction significantly prevails at the site. The division of the weighted concentration roses according to the mixing layer height does not describe the PM₁₀ concentrations and the wind direction at a certain MLH, but a situation at a ground measurement height at the site and during the time when the mixing layer height reached the described height.

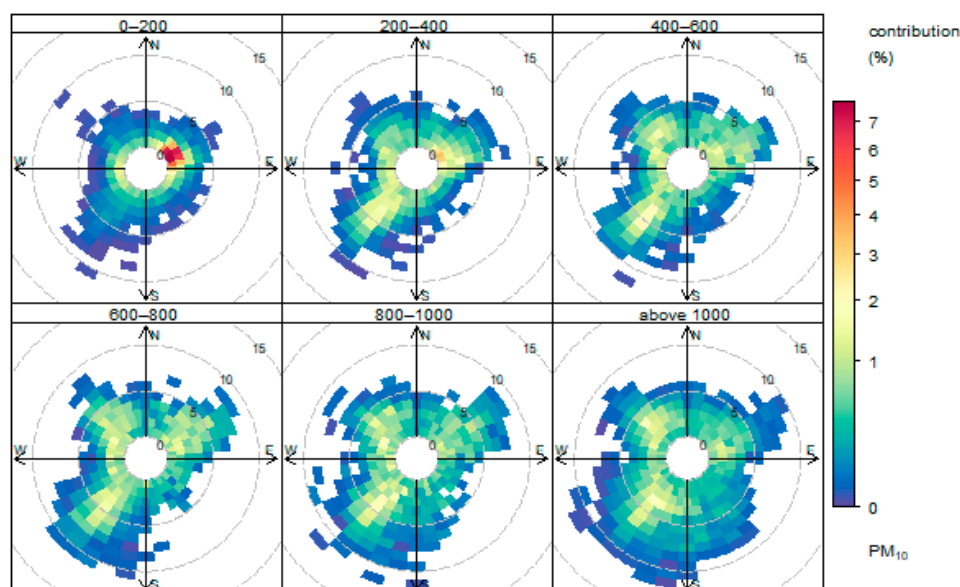


Figure 18. A weighted PM₁₀ concentration rose divided according to the mixing layer height, the Věřňovice site, 2016–2019.

When comparing Figures 14, 17 and 18, a difference in the layout of the frequency of counts of wind directions between both sites becomes apparent. While at the Třinec-Kosmos site, a boundary of the prevailing wind direction along the southeast/northwest axis is more sharply visible in the pictures, at Věřňovice, despite the fact that the prevailing wind direction is along the southwest/northeast axis, the frequencies of counts of directions are spread more evenly to the other sectors, as well. This situation corresponds to the information described in Chapters 1 and 2.

The concentration roses (Figure 19) for 2016–2019 show that the maximum PM₁₀ concentration contributions come to the Třinec-Kosmos site at a low MLH level of up to 200 m and low wind speeds of up to 1 m·s⁻¹ from the northern (N) to the western (W) sector. For MLHs of 200–400 m, an influence of the wind direction from the E sector is also significantly shown, as well as the influence from the N and W sectors. The average maximum PM₁₀ concentration contributions at the site occur at MLHs of up to 400 m above the ground and at wind speeds of up to 2 m·s⁻¹. On the occurrence of a higher MLH level of up to 600 m, a higher wind speed of above 4 m·s⁻¹ from the N and NE directions contributes to the resulting situation more significantly. From the point of view of the PM₁₀ concentration roses divided according to the mixing layer height for the Třinec-Kosmos site, it is possible to regard the SW wind directions as those directions with the lowest PM₁₀ contribution; at higher wind speeds of above 4 m·s⁻¹, the S–SE directions also contribute the lowest amount.

Figure 20 illustrates concentration roses for the Věřňovice site for 2016–2019, which are divided according to the different heights of the mixing layer. The highest PM₁₀ concentration contributions are reached up to the occurrence of MLHs of 200 m above the ground at wind speeds of up to 2 m·s⁻¹ from the E–NE. The influence of the wind from these directions is shown in the average maximum PM₁₀ contributions up to the height of 600 m, during which time the influence of a rising wind speed of up to about 6 m·s⁻¹ also increases proportionally.

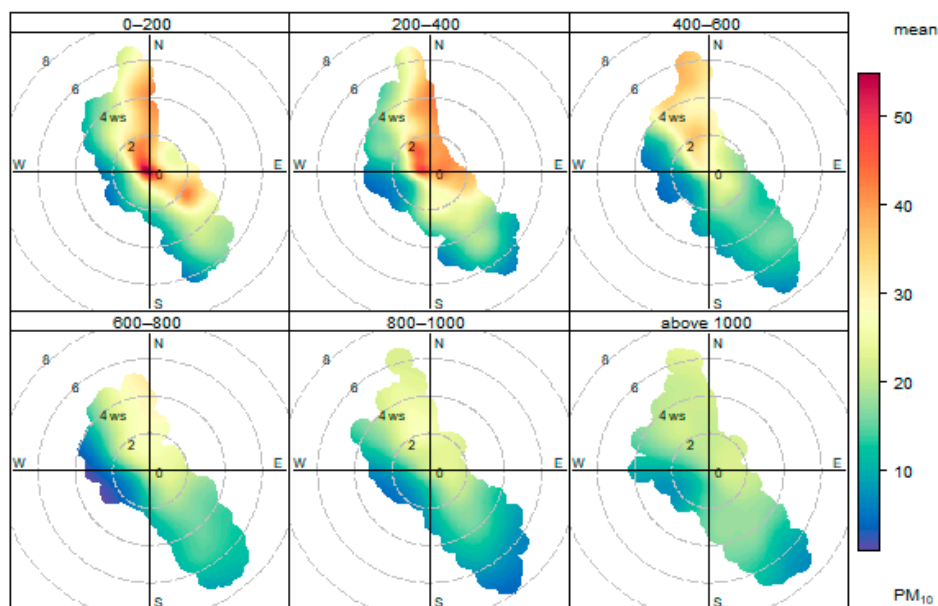


Figure 19. Average PM_{10} concentration roses divided according to the mixing layer height, Třinec-Kosmos site, 2016–2019.

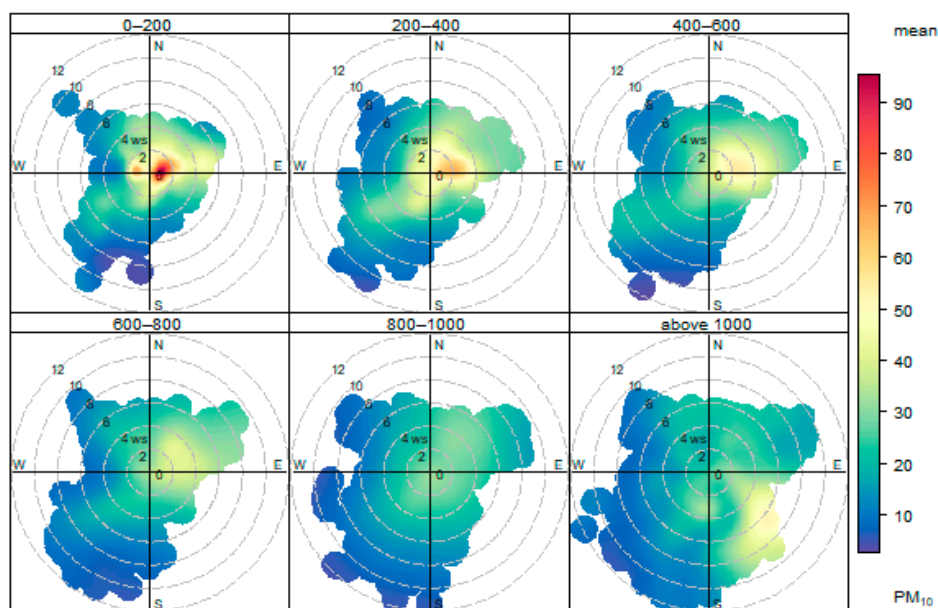


Figure 20. Average PM_{10} concentration roses divided according to the mixing layer height, the Věřňovice site, 2016–2019.

When comparing the PM_{10} concentration contributions at the sites after the division according to the wind directions and according to the MLH levels (Figures 15–20), it is apparent that at higher MLHs the contributions generally reach lower values for all wind directions.

4. Discussion

The detection of dependences of PM_{10} concentrations on the mixing layer height may point out at possible pollution sources in the area; it would, however, be necessary to check the exact determination of the source type by other methods used in assessing the field of air quality, e.g., by more detailed air pollutant measurements and by methods for pollution source identification, e.g., Positive Matrix Factorization (PMF) [53] and back trajectories [54]. The high PM_{10} concentrations in combination with the low mixing layer height provide information about the high influence of low-emitting sources of

air pollution (individual heating) on the air quality at a given site. On the other hand, higher PM₁₀ concentrations reached at higher MLH levels show the influence of industrial sources, sources with emission release at greater heights. High concentrations combined with a low wind speed, perhaps even with no wind, show the influence of sources in the vicinity of the site. Conversely, higher wind speeds combined with high PM₁₀ concentrations correspond to the premise of transport from more remote places to the site [16,17,24–26].

The findings of this work correspond to the conclusions of Air Quality Improvement Program [52] elaborated for both sites and areas of interest in which the sites are located and also to the “Air Pollution Sources Contribution to PM_{2.5} Concentration in the Northeastern Part of the Czech Republic” analysis [55].

As mentioned before in Section 2, the meteorological variables data used the analysis from the ground measurements of temperature at a height of 2 m above the ground; the wind direction and speed were measured at 10 m above the ground. The values of these variables at various mixing layer heights were not included in the analysis. A vertical wind direction and speed and temperature profile would be a significant addition to the assessment that would, among other things, provide information about the occurrence of temperature inversions. This information could be completed with distant measurement data or from model calculations in a subsequent assessment. It is necessary to point out again that the ceilometer measurement is biased by noise at the lowest level above the ground [46], which interferes up to roughly 50 m according to the existing available sources.

Although the PM₁₀ concentrations are significantly dependent both on the wind speed and the mixing layer height, the dependence of the wind speed and MLH does not show a significant statistical dependence. The differences are also apparent between both assessed sites with a statistically higher dependence detected at the Věřňovice site. Orography is assumed to play an important role in this aspect (Section 2). While the Věřňovice site is situated in open terrain, the Třinec-Kosmos site is situated in an urban development at the end of Jablunkov Furrow at the foothills of the Moravian-Silesian Beskydy mountains.

Correlation dependences for the wind direction and MLH have not been elaborated. The authors do not consider this aspect important. The prevailing wind direction is different at both sites, the difference lying mostly in the area geomorphology where the sites are situated. The authors find the wind direction and speed assessment sufficiently useful, divided according to the MLHs mentioned in this article. These indicators serve primarily for detection of the origin and location of possible pollution sources that influence the given area.

Another opportunity for analysis is the assessment of other pollutants' dependence on the mixing layer height. Among the examples are ground-level ozone and processing for the warm part of the year [56], as well as a more detailed assessment of the behavior of pollutants such as sulfur dioxide, nitrogen dioxide, and suspended particles during winter smog situations when there is a low mixing layer height [32].

The disadvantage of an assessment of the relationships between meteorology and ambient air quality with regard to the mixing layer height lies in the fact that there are no available data from a longer sequence of ceilometer measurement. The assessment of the mixing layer height trends from a long-term point of view would surely bring additional information about the development or changes of the dispersion conditions, especially in the areas with poor air quality. The observed information may serve as a basis for the evaluation of current situations with high PM₁₀ concentrations, for announcing and invalidating smog situations, and model solutions of pollution situation forecasts.

5. Conclusions

The presented analysis provides evidence of the influence of the mixing layer height, combined with other meteorological variables, on PM₁₀ concentrations in the area of the Czech-Polish border, which faces problems with a complex representation of a substantial number of various pollution

source types. The influence on the pollution situation in combination with meteorological variables at a given site also differs depending on the varied geographical conditions.

The influence of a temperature below 1 °C on the pollution situation is noticeable at both sites. The highest numbers of exceedances of PM₁₀ daily concentrations of 50 µg·m⁻³ occur at low temperatures combined with a mixing layer height of up to 300 m. In the case of Třinec-Kosmos, the average PM₁₀ concentrations at temperatures below 1 °C reach the highest values on the occurrence of a mixing layer height of up to 300 to 400 m. The decrease in PM₁₀ concentrations with increasing MLHs at temperatures below 1 °C is not very significant. In this case, the influence of a rising height of the mixing layer at temperatures below 1 °C on the average PM₁₀ concentrations is not as significant as in the case of Věřňovice, where a difference of several tens of µg·m⁻³ in the average PM₁₀ concentrations is observed between levels of up to 200 m, and levels of 200–300 m.

The influence of the wind speed on the occurrence of various MLHs on PM₁₀ concentrations is also noticeable. The average PM₁₀ hourly concentrations at Třinec-Kosmos are the highest at wind speeds of up to 0.2 m·s⁻¹, or 0.5 m·s⁻¹, at MLH levels of up to almost 600 m, at Věřňovice the influence of wind speeds of up to 2 m·s⁻¹ is detected. In both cases, throughout the assessment of the number of PM₁₀ daily concentrations above 50 µg·m⁻³, it is then clear that higher values occur in the case of Třinec at wind speeds of 0.5 up to 2 m·s⁻¹ and MLHs of 200–300 m. At the Věřňovice station, the highest number of limit value exceedances was observed at wind speeds between 1–2 m·s⁻¹ and at wind speeds above 2 m·s⁻¹ and MLHs of 200–300 m.

The influence of the wind direction combined with the MLH is different at both sites; however, it is crucial as well. Despite the fact that the most frequent PM₁₀ contributions come to the Třinec-Kosmos site from the SE direction, the average maximum concentration contributions come from the W–N sectors at low wind speeds and MLHs of up to 400 m. In Věřňovice, regardless of the prevailing SW wind direction, sources in the NE–E sector from the site have a crucial influence on the air pollution level caused by PM₁₀. The maximum PM₁₀ contributions are reached on the occurrence of MLHs of up to 200 m at Věřňovice station.

Author Contributions: Conceptualization, V.V. and D.H.; methodology, V.V. and D.H.; formal analysis, V.V. and D.H.; investigation, V.V. and D.H.; resources, V.V. and D.H.; data curation, D.H. and V.V.; writing—original draft preparation, V.V.; writing—review and editing, D.H. and V.V.; visualization, D.H. and V.V.; supervision, V.V. and D.H.; project administration, V.V. All authors have read and agreed to the published version of the manuscript.

Funding: This research received no external funding.

Acknowledgments: The data for the analysis were provided by the Czech Hydrometeorological Institute (www.chmi.cz). The assessment is based on measurements at the sites run by the Czech Hydrometeorological Institute.

Conflicts of Interest: The authors declare no conflicts of interest.

References

1. WHO. *Health Effects of Particulate Matter*, 2nd ed.; Policy Implications for Countries in Eastern Europe, Caucasus and Central Asia; WHO Regional Office for Europe: Copenhagen, Denmark, 2013; ISBN 978-92-890-0001-7.
2. WHO. Ambient (Outdoor) Air Pollution. Available online: [https://www.who.int/en/news-room/fact-sheets/detail/ambient-\(outdoor\)-air-quality-and-health](https://www.who.int/en/news-room/fact-sheets/detail/ambient-(outdoor)-air-quality-and-health) (accessed on 2 February 2020).
3. Kampa, M.; Castanas, E. Human health effects of air pollution. *Environ. Pollut.* **2008**, *151*, 362–367. [[CrossRef](#)] [[PubMed](#)]
4. Schwartz, J. Air Pollution and Blood Markers of Cardiovascular Risk. *Environ. Health Perspect.* **2001**, *109*, 405–409. [[PubMed](#)]
5. Pope, C.A.; Dockery, D.W. Health Effects of Fine Particulate Air Pollution: Lines that Connect. *J. Air Waste Manag. Assoc.* **2006**, *56*, 709–742. [[CrossRef](#)]
6. EEA. *Air quality in Europe—2019 Report*, 1st ed.; Publications Office of the European Union: Copenhagen, Denmark, 2019; ISBN 978-92-9480-088-6.

7. IQ Air. World Most Polluted Cities 2019 (PM2.5). Available online: <https://www.iqair.com/world-most-polluted-cities> (accessed on 30 March 2020).
8. Prášek, J. *Změny Geografického Prostředí v Pohraničních Oblastech Ostravského a Hornoslezského Regionu (Changes in the Geographical Environment in the Border Regions of the Ostrava and Upper Silesian Regions)*; Ostravská Univerzita: Ostrava, Czech, 1998; Volume 1. (In Czech)
9. Prokop, R. Historická hranice Moravy a Slezska ve vývoji ostravské aglomerace (Historical boundary of Moravia and Silesia in the development of the Ostrava agglomeration). *Geogr. Rozhl.* **1996**, *6*, 4–5. (In Czech)
10. Šindler, P. Vývojové tendence sídelní struktury česko-polského pohraničí na příkladu severní Moravy a českého Slezska (Trends in the settlement structure of the Czech-Polish borderland on the example of North Moravia and Czech Silesia). *Geogr. Rozhl.* **1996**, *6*, 11–13. (In Czech)
11. EC. *Directive 2004/107/EC of the European Parliament and of the Council of 15 December 2004 Relating to Arsenic, Cadmium, Mercury, Nickel and Polycyclic Aromatic Hydrocarbons in Ambient Air*; EC: Brussel, Belgium, 2005.
12. EC. *Directive 2008/50/EC of the European Parliament and of the Council of 21 May 2008 on Ambient Air Quality and Cleaner Air for Europe*; EC: Brussel, Belgium, 2008.
13. Zákon č. 201/2012 Sb. ze dne 2. května 2012 o Ochráně Ovzduší (Act No. 201/2012 Coll. of 2 May 2012 on Air Protection); Tiskárna Ministerstva vnitra: Praha, Czech, 2012; pp. 2785–2848. (In Czech)
14. Hůnová, I. Ambient Air Quality in the Czech Republic: Past and Present. *Atmosphere* **2020**, *11*, 214. [[CrossRef](#)]
15. *Znečištění Ovzduší na Území České Republiky v Roce 2018 (Air Pollution in the Territory of the Czech Republic in 2018)*, 1st ed.; Czech Hydrometeorological Institute: Prague, Czech, 2019; ISBN 978-80-87577-95-0. (In Czech)
16. Bednář, J. *Meteorologie (Meteorology)*, 1st ed.; Úvod do Studia Dějů v Zemské Atmosféře (Introduction to the Study of Events in the Earth's Atmosphere); Portál: Praha, Czech, 2003; ISBN 80-7178-653-5. (In Czech)
17. Rein, F. Znečištění ovzduší a mezní vrstva atmosféry z hlediska klimatologie (Air pollution and atmospheric boundary layer in terms of climatology). *Meteorol. Zprávy* **1971**, *24*, 74–79. (In Czech)
18. Novák, M. *Meteorologie a Ochrana Prostředí*, 1st ed.; Úvod do Meteorologie a Klimatologie (Meteorology and Environmental Protection; Introduction to Meteorology and Climatology); Univerzita Jana Evangelisty Purkyně, Fakulta Životního Prostředí: Ústí nad Labem, Czech, 2004; ISBN 80-7044-597-1. (In Czech)
19. Jaňour, Z. *Modelování Mezní Vrstvy Atmosféry (Atmospheric Boundary Layer Modeling)*, 1st ed.; [Učební Text pro Posluchače Matematicko-Fyzikální Fakulty UK] [Textbook for Students of Faculty of Mathematics and Physics of Charles University]; Karolinum: Praha, Czech, 2001; ISBN 80-246-0330-6. (In Czech)
20. Keder, J.; Škáchová, H. *Hodnocení Rozptylových Podmínek pro Šíření Znečišťujících Látek Pomocí Ventilačního Indexu (Evaluation of Dispersion Conditions for the Diffusion of Pollutants Using the Ventilation Index)*; Vodní Zdroje Ekomonitor: Chrudim, Czech, 2011; pp. 19–23. (In Czech)
21. Baláková, L.; Škáchová, H.; Crhová, L. *Kvalita Ovzduší a Rozptylové Podmínky na Území ČR (Air Quality and Dispersion Conditions in the Czech Republic)*; Czech Hydrometeorological Institute: Prague, Czech, 2018. (In Czech)
22. Czernecki, B.; Pótrolniczak, M.; Kolendowicz, L.; Marosz, M.; Kendzierski, S.; Pilgaj, N. Influence of the atmospheric conditions on PM10 concentrations in Poznań, Poland. *J. Atmos. Chem.* **2017**, 115–139. [[CrossRef](#)]
23. Stull, R.B. *An Introduction to Boundary Layer Meteorology*, 1st ed.; Atmospheric and Oceanographic Sciences Library; Springer: Boston, MA, USA, 1988; ISBN 90-277-2769-4.
24. Blažek, Z.; Černikovský, L.; Krajny, E.; Krejčí, B.; Ošrůdka, L.; Volná, V.; Wojtylak, M. *Vliv Meteorologických Podmínek na Kvalitu Ovzduší v Přeshraniční Oblasti Slezska a Moravy (Influence of Meteorological Conditions on Air Quality in the Cross-Border Region of Silesia and Moravia)*, 1st ed.; Český Hydrometeorologický Ústav: Praha, Czech, 2013. (In Czech)
25. Blažek, Z.; Černikovský, L.; Krejčí, B.; Volná, V. Air Silesia—Meteorologicko-imisní vztahy a odhad transhraničního přenosu (Air Silesia—meteorological and air pollution relations and estimation of transboundary transmission). *Ochr. Ovzduší* **2014**, *26*, 53–61. (In Czech)
26. Blažek, Z.; Černikovský, L.; Krejčí, B.; Volná, V. Transboundary Air-Pollution Transport in the Czech-Polish Border Region between the Cities of Ostrava and Katowice. *Cent. Eur. J. Public Health* **2016**, *24*, 45–50.
27. Barmpadimos, I.; Hueglin, C.; Keller, J.; Henne, S.; Prévôt, A.S.H. Influence of meteorology on PM10 trends and variability in Switzerland from 1991 to 2008. *Atmos. Chem. Phys.* **2011**, *11*, 1813–1835. [[CrossRef](#)]
28. Reizer, M.; Juda-Rezler, K. Explaining the high PM₁₀ concentrations observed in Polish urban areas. *Air Qual. Atmos. Health* **2016**, *9*, 517–531. [[CrossRef](#)]

29. Volná, V.; Blažek, Z.; Krejčí, B. Zimní smogové situace na Ostravsku a Olomoucku v letech 2001–2016 (Winter smog situations in the Ostrava and Olomouc Regions in 2001–2016). *Meteorol. Zprávy* **2018**, *71*, 86–92. (In Czech)
30. Molnár, A.; Bécsi, Z.; Imre, K.; Gácsér, V.; Ferenczi, Z. Characterization of Background Aerosol Properties during a Wintertime Smog Episode. *Aerosol Air Qual. Res.* **2016**, *16*, 1793–1804. [[CrossRef](#)]
31. CHMI. Pravidla Fungování Smogového Varovného a Regulačního Systému (Rules of Operation of Smog Warning and Regulation System). Available online: http://portal.chmi.cz/files/portal/docs/uoco/smog/SVRS_pravidla-fungovani.pdf (accessed on 18 February 2020). (In Czech)
32. Volná, V.; Hladký, D. Koncentrace suspendovaných částic PM₁₀ a výška směšovací vrstvy v Moravskoslezském kraji během chladných sezón 2016/2017 a 2017/2018 (Concentrations of suspended particles PM₁₀ and mixing layer height in the Moravian-Silesian Region during the cold seasons 2016/2017 and 2017/2018). *Meteorol. Zprávy* **2019**, *72*, 77–87. (In Czech)
33. Oleniacz, R.; Bogacki, M.; Szulecka, A.; Rzeszutek, M.; Mazus, M. Assessing the impact of wind speed and mixing-layer height on air quality in Krakow (Poland) in the years 2014–2015. *JCEEA* **2016**, *33*, 315–342. [[CrossRef](#)]
34. Geiß, A.; Eiegner, M.; Bonn, B.; Schäfer, K.; Forkel, R.; von Schneidmesser, E.; Münkel, C.; Chan, K.L.; Nothard, R. Mixing layer height as an indicator for urban air quality? *Atmos. Meas. Tech.* **2017**, *10*, 2969–2988. [[CrossRef](#)]
35. Schäfer, K.; Emeis, S.; Hoffman, H.; Jahn, C. Influence of mixing layer height upon air pollution in urban and sub-urban areas. *Meteorol. Z.* **2006**, *15*, 647–658. [[CrossRef](#)]
36. Wagner, P.; Schäfer, K. Influence of mixing layer height on air pollutant concentrations in an urban street canyon. *Urban Clim.* **2017**, *22*, 64–79. [[CrossRef](#)]
37. Holst, J.; Mayer, H.; Holst, T. Effect of meteorological exchange conditions on PM₁₀ concentration. *Meteorol. Z.* **2008**, *17*, 273–282. [[CrossRef](#)]
38. Tiwari, S.; Dumka, U.C.; Gautam, A.S.; Kaskaoutis, D.G.; Srivastava, A.K.; Bisht, D.S.; Chakrabarty, R.K.; Sumlin, B.J.; Solmon, F. Assessment of PM_{2.5} and PM₁₀ over Guwahati in Brahmaputra River Valley. *Atmos. Pollut. Res.* **2017**, *8*, 13–28. [[CrossRef](#)]
39. Zhao, H.; Che, H.; Ma, Y.; Wang, Y.; Yang, H.; Liu, Y.; Wang, Y.; Wang, H.; Zhang, X. The Relationship of PM Variation with Visibility and Mixing-Layer Height under Hazy/Foggy Conditions in the Multi-Cities of Northeast China. *Int. J. Environ. Res. Public Health* **2017**, *14*, 471. [[CrossRef](#)] [[PubMed](#)]
40. Czech Hydrometeorological Institute. Available online: <http://portal.chmi.cz/> (accessed on 18 February 2020).
41. CHMI. Trinec-Kosmos. Available online: http://portal.chmi.cz/files/portal/docs/uoco/web_generator/locality/pollution_locality/loc_TTRO_CZ.html (accessed on 18 February 2020).
42. CHMI. Věřňovice. Available online: http://portal.chmi.cz/files/portal/docs/uoco/web_generator/locality/pollution_locality/loc_TVER_CZ.html (accessed on 18 February 2020).
43. MŽP. Sdělení Odboru Ochrany Ovzduší, Kterým se Stanoví Seznam Stanic Zahnutých Do Státní Sítě Imisního Monitoring (Communication from the Air Protection Department, Which Establishes a List of Stations Included in the National Air Pollution Monitoring Network). Available online: http://portal.chmi.cz/files/portal/docs/uoco/oez/emise/evidence/aktual/Vestnik_2016_1.pdf (accessed on 22 March 2020). (In Czech)
44. CHMI. Air Pollution and Atmospheric Deposition in Data, the Czech Republic, 2018. Summary Tabular Survey. Available online: http://portal.chmi.cz/files/portal/docs/uoco/isko/tab_roc/2018_enh/index_CZ.html (accessed on 20 March 2020).
45. Vaisala. Available online: <https://www.vaisala.com/en> (accessed on 11 January 2020).
46. Kotthaus, S.; O'Connor, E.; Münkel, C.; Charlton-Perez, C.; Haefelin, M.; Gabey, A.M.; Grimmond, C.S.B. Recommendations for processing atmospheric attenuated backscatter profiles from Vaisala CL31 ceilometers. *Atmos. Meas. Tech.* **2016**, *9*, 3769–3791. [[CrossRef](#)]
47. Carslaw, D.C.; Ropkins, K. Openair—An R package for air quality data analysis. *Environ. Model. Softw.* **2012**, *27–28*, 52–61. [[CrossRef](#)]
48. CHMI. *Znečištění Ovzduší na Území České Republiky v Roce 2015 (Air Pollution in the Czech Republic in 2015)*, 1st ed.; Český Hydrometeorologický Ústav: Praha, Czech, 2016; ISBN 978-80-87577-60-8. (In Czech)
49. ŘSD ČR. Intenzity Dopravy na Dálnicích a Silnicích I. Třídy v ČR v Roce 2010. Available online: <https://www.rsd.cz/wps/wcm/connect/b63a9557-7496-478a-8ef3-80629d92f954/pentlogram-2010.jpg?MOD=AJPERES> (accessed on 28 March 2020).

50. Czudek, T. *Reliéf Moravy a Slezska v Kvartéru (Relief of Moravia and Silesia in Quaternary)*, 1st ed.; Sursum: Tišnov, Czech, 1997; ISBN 80-85799-27-8. (In Czech)
51. Weissmannová, H. *Ostravsko*, 1st ed.; Agentura Ochrany Přírody a krajiny ČR: Praha, Czech, 2004; ISBN 80-86064-67-0. (In Czech)
52. MŽP. *Air Quality Improvement Program of Agglomeration Ostrava/Karviná/Frýdek-Místek—CZ08A*; MŽP: Praha, Czech, 2016.
53. Norris, G.; Duvall, R.; Brown, S.; Bai, S. *EPA Positive Matrix Factorization (PMF) 5.0 Fundamentals and User Guide*; US EPA: Washington, DC, USA, 2014.
54. Stein, A.F.; Draxler, R.R.; Rolph, G.D.; Stunder, B.J.B.; Cohen, M.D.; Ngan, F. NOAA's HYSPLIT Atmospheric Transport and Dispersion Modeling System. *Bull. Am. Meteorol. Soc.* **2015**, *96*, 2059–2077. [[CrossRef](#)]
55. Seibert, R.; Nikolova, I.; Volná, V.; Krejčí, B.; Hladký, D. Air Pollution Sources Contribution to PM_{2.5} Concentration in Northeastern Part of the Czech Republic. *Atmosphere* **2020**. under review.
56. Komínková, K.; Holoubek, I. *Využití Dat z Ceilometru při Interpretaci Vývoje Koncentrací Látek v O vzduší Během Dne (Use of the Ceilometer Data to Explainig Changes in Pollutants Concetration Gradient in the Air during the Day)*; Masarykova Univerzita: Brno, Czech, 2017; pp. 198–202. (In Czech)



© 2020 by the authors. Licensee MDPI, Basel, Switzerland. This article is an open access article distributed under the terms and conditions of the Creative Commons Attribution (CC BY) license (<http://creativecommons.org/licenses/by/4.0/>).